Helix Packing in Subunit *a* of the *Escherichia coli* ATP Synthase as Determined by Chemical Labeling and Proteolysis of the Cysteine-Substituted Protein†

Di Zhang‡ and Steven B. Vik*

Department of Biological Sciences, Southern Methodist University, Dallas, Texas 75275-0376

Received August 15, 2002; Revised Manuscript Received October 16, 2002

ABSTRACT: Subunit *a* of the *Escherichia coli* ATP synthase is thought to control access of protons to the ring of *c* subunits during proton-driven ATP synthesis. In this study, the surface exposure of subunit *a* in the periplasm has been examined using 3-*N*-maleimidyl-propionyl biocytin labeling in cells permeabilized by polymyxin B nonapeptide, and the helix packing at the periplasmic surface has been probed by metal-chelate mediated proteolysis. Eighteen residues between 119 and 146 were changed individually to cysteine and tested for accessibility. Positions labeled included D124 and D146, indicating a periplasmic loop of at least 23 amino acids. Residues near the ends of the transmembrane spans were tested with 5-(α-bromoacetamido)-1,10-phenanthroline-copper for chemical proteolysis. Only residues W241C and D44C, and to a lesser extent I43C, led to proteolytic fragments after oxidation. The fragments were sized by comparison with molecular weight standards generated by Factor Xa sites engineered into subunit *a*. Fragments were detected by immunoblotting using an engineered HA epitope at the carboxyl-terminal end of subunit *a*. The results indicated that both transmembrane span 5 (W241) and transmembrane span 1 (D44) are close to transmembrane span 2.

The ATP synthase from *Escherichia coli* is typical of the enzymes found in mitochondria, chloroplasts, and many other bacteria that synthesize ATP (For a recent review see ref *1*). It is composed of two sub-complexes: an F_1 sector with subunits that contain the catalytic sites, and a membrane-bound F_o sector, with subunits that conduct protons across the membrane. In the *E. coli* enzyme, five different subunits are found in F_1: α, *β*, *γ*, *δ*, and *ϵ*, with a stoichiometry of 3:3:1:1:1. In the F_o sector, three different subunits are found: *a*, *b*, and *c*, with a stoichiometry of 1:2:9−12 (*2*).

Mechanistically, the enzyme functions as a rotary motor and the subunits can be divided into rotor and stator subunits. The rotor includes *γ*, *ϵ*, and *c* subunits. The stator subunits include *δ*, *a*, and *b*, which anchor the catalytic sites found in α and *β* to the membrane. The mechanism by which the proton motive force across the membrane drives ATP synthesis involves the rotation of the *c* oligomer of F_o along with subunits *γ* and *ϵ*. High-resolution structures of F_1, primarily from bovine mitochondria, have provided details about the catalytic sites and their conformational changes (*3*−*5*). Evidence for rotation of subunits through 360° in response to ATP hydrolysis has been provided by direct observation of fluorescently labeled actin filaments attached to *γ* or *ϵ* (*6*−*8*).

A high-resolution structure of the F_o sector is not yet available. Subunit *b* is thought to be embedded in the membrane via a hydrophobic region near its N-terminus. Various studies have shown that a truncated, soluble form of *b* is extended and dimeric (*9*−*13*). Likewise, studies of an N-terminal fragment, using NMR and disulfide formation, have shown it to be α-helical and dimeric (*14*). NMR studies of the monomeric *c* subunit have shown it to be an α-helical hairpin with two transmembrane spans connected by a short polar loop (*15*). The number of *c* subunits that make up the oligomer in F_o from *E. coli* is still uncertain, but atomic force microscopy applied to F_o from other species has provided evidence for a ring of *c* subunits (*16*, *17*). The likely stoichiometry for *a*:*c* in the *E. coli* F_o is 1:10 (*18*).

Other experimental approaches have been employed in the analysis of subunit *a*, to understand its arrangement in the membrane and its relationship to the other subunits of the F_1F_0 ATP synthase. In previous studies, surface labeling of unique, engineered cysteine residues was used to establish the number of transmembrane spans and to characterize the first cytoplasmic loop of subunit *a* (*19*−*22*). These results are summarized in Figure 1, in which five transmembrane spans are shown, and the first cytoplasmic loop is drawn to reflect the limited accessibility of its central region. Residues important for function (*23*−*26*) have been shown to reside in transmembrane spans 4 and 5. Cross-linking studies have shown that transmembrane span 4 of subunit *a*, between residues 207 and 225, appears to be in contact with subunit *c* (*27*) and that residues 74 and 91 of the first cytoplasmic loop are in close proximity to subunit *b* (*22*). Transmembrane span 4 includes *a*R210, which is strictly conserved among

† Support for this study was provided by grants from NIH (GM40508) and The Welch Foundation (N-1378)

* Correspondeing author. Address: Department of Biological Sciences, 6501 Airline Road, Southern Methodist University, Dallas, TX 75275-0376. Telephone: (214) 768-4228. Fax: (214) 768-3955. E-mail: svik@mail.smu.edu.

‡ Current address: BioPort Corporation, Lansing, MI 48906.

[1] Abbreviations: BAP, 5-(α-bromoacetamido)-1,10-phenanthroline; HA epitope, mouse hemagglutinin epitope; MPB, 3-*N*-maleimidyl-propionyl biocytin; Ni−NTA, nickel−nitrilotriacetic acid; PMBN, polymyxin B nonapeptide; PVDF, poly(vinylidene difluoride); TBS, 20 mM Tris-HCl (pH 7.5) and 500 mM NaCl.

10.1021/bi026649t CCC: $25.00
Published on Web 12/17/2002

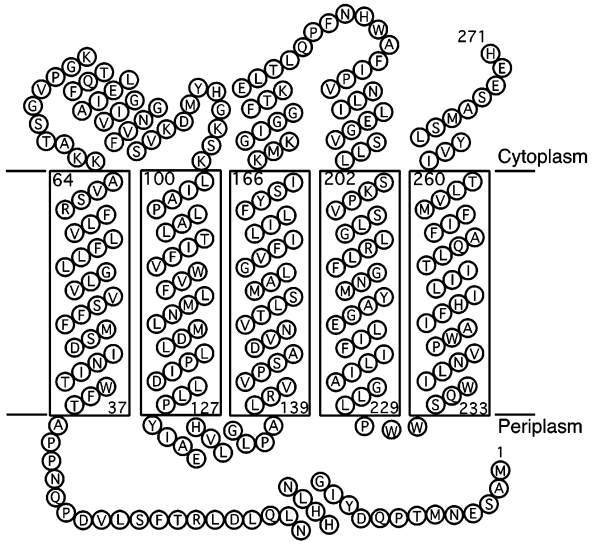

FIGURE 1: The transmembrane model of subunit *a*. The cytoplasmic loop between residues 64 and 100 is drawn to indicate that the central region has limited accessibility to the reagent MPB, but the segments nearest the membrane are highly exposed.

all known species, and in *E. coli* any mutation at this position results in inability to grow on succinate minimal medium and in loss of ATP driven proton translocation. It is likely that *a*R210 interacts with the essential residue *c*D61 during coupled proton translocation. The mechanism by which subunit *a* contributes to the proton conducting path of the ATP synthase is not clear, but it seems to play an essential role in this function. A model has been presented in which subunit *a* contributes amino acids that make up two-half-channels, one opening to the periplasm and one to the cytoplasm, that allow access to the proton binding site on subunit *c* (*28*).

Information about the interactions between the transmembrane spans of subunit *a* will contribute to an understanding of the possible proton pathways through subunit *a* to subunit *c*. So far, such evidence (*20*, *23*, *29*, *30*) has consisted of a series of second-site suppressors of mutations in subunit *a*. Second site suppression can occur through either direct or indirect interactions. In this study these suppressors are evaluated for possible proximity by using accessibility to the reagent MPB to distinguish between residues that are in loops and those that are in transmembrane spans. Furthermore, a chemical protease approach was used in which cysteinyl residues were derivatized with 5-(α-bromoacetamido)-1,10-phenanthroline-copper, a reagent capable of generating proteolysis at sites in the protein that are nearby in space (*31*). In this way it is possible to identify relationships between transmembrane spans with respect to both proximity and orientation.

EXPERIMENTAL PROCEDURES

Materials. Restriction enzymes and Factor Xa were obtained from New England Biolabs. Synthetic oligonucleotides were obtained from Operon Technologies. DNA sequencing was done by Lone Star Labs. MPB and BAP were obtained from Molecular Probes. Nickel−nitrilotriacetic acid (Ni−NTA) resin and DNA miniprep kits were obtained from Qiagen. Mouse anti-HA antibody was obtained from Roche. Goat anti-mouse IgG-alkaline phosphatase conjugate, goat anti-rabbit IgG-alkaline phosphatase conjugate, avidin-conjugated alkaline phosphatase, 5-bromo-4-chloro-3-indoylphosphate-*p*-toluidine salt (BCIP), *p*-nitro blue tetrazolium chloride (NBT), SDS−polyacrylamide gels, PVDF membranes, and lo- and broad range protein molecular weight standards were obtained from Bio-Rad. *N*-Octyl-β-D-glucoside was purchased from Anatrace. All other chemicals were purchased from Sigma or Fisher.

Plasmids, Mutagenesis, Growth, and Expression. The plasmids, pLN6HisHA (*19*), pLN7HisHA (*22*), pTW1HisHA (*19*), pARP2HisHA (*21*), pLN46HisHA, and pDZ46HisHA were used for the construction of mutants. They differ primarily in the placement of unique restriction sites that are necessary for cassette mutagenesis. Plasmid pLN46HisHA was constructed by ligating the 1081 base pair Pst I-EcoR I fragment from pLN6HisHA to the 2251 base pair Pst I-EcoR I fragment from pLN46His (*19*). Plasmid pLN46HisHA has an extra AT inserted in codon 161(ATC) to generate a unique EcoR V site (GAATTC) for cassette mutagenesis. Plasmid pDZ46HisHA is a wild-type version of pLN46HisHA that was constructed by replacing the 16 base pair Avr II-EcoR V fragment with a synthetic fragment lacking an AT at the blunt end that would be necessary to regenerate the EcoR V site. These plasmids all produce a subunit *a* that includes an HA epitope (YPYDVPDYA), derived from the hemagglutinin protein of human influenza virus, and a His_6 tag at the C-terminus of the protein. These tags have no effect on function. Amino acid substitutions were carried out using cassette mutagenesis (*32*). For expression, RH305 (*unc*B205, *rec*H56, *srl*::Tn10, *bgi*R, *thi*-1, *rel*-1, HfrPO1) was used as the background strain (*33*). It produces a subunit *a* that is truncated near Pro-240 (*34*), but is nonfunctional and cannot be detected in cell extracts. It is complemented by plasmids containing the wild type *unc*B gene coding for subunit *a*, such as those listed above. For subcloning and mutagenesis, XL1-Blue (*rec*A1, *end*A1, *gyr*A96, *thi*, *hsd*R17 (r_k-, m_k+), *sup*E44, *rel*A1, λ^-, (*lac*), {F′m *pro*AB, *lac*I^q ZΔM15, Tn 10 (tet^r)}) was used. Cultures were grown, and inside-out membrane vesicles were prepared from 250 mL cultures according to previous procedures (*19*). MPB labeling of whole cells was carried out as described previously (*21*).

Cleavage of Subunit a in Whole Cells. A 30 mL culture of cells was grown in LB medium at 37 °C to $A_{600} = 1.0$ and harvested. The cells were suspended in 200 mM Tris-HCl (pH 7.4) and washed twice. They were resuspended in 0.5 mL of the same buffer with 50 μM PMBN and 50 μM BAP and incubated at room temperature for 1 h. After centrifugation for 10 min at 8500 rpm at 4 °C, the cells were washed three times with same buffer. Then the cells were suspended in 0.5 mL of the same buffer with 50 μM of $CuSO_4$ and incubated at room temperature for 20 min. The cells were washed three times again. After resuspension in 0.5 mL of the same buffer, the reaction was activated by adding 30 mM ascorbate (pH 7.4) and 1 μL of 30% H_2O_2. The reaction was stopped after 20 min by washing the cells as before. The cells were suspended in 200 mM Tris-HCl (pH 7.4), 1.5% octyl-glucoside, 0.1% deoxycholate, 0.5% cholate, and 0.5% Tween 20. Following a 2 h incubation at 4 °C, the subunit *a* was purified using Ni−NTA resin, as described below.

Cleavage of Subunit a in Detergent Solution. A 30 mL culture of cells was grown in LB medium at 37 °C to A_{600}

= 1.0 and harvested. The cells were suspended in 200 mM Tris-HCl (pH 7.4), washed twice, and resuspended in 1 mL of 200 mM Tris-HCl (pH 7.4), 1.5% octyl-glucoside, 0.1% deoxycholate, 0.5% cholate and 0.5% Tween 20. After 2 h incubation at 4 °C, the cells were centrifuged for 10 min at 14 000 rpm at 4 °C. The supernatant was transferred to a new microfuge tube and BAP was added to a final concentration of 50 μM. After incubation for 60 min at room temperature, the samples were centrifuged for 1 min at 14 000 rpm at 4 °C. The supernatant was transferred to a new microcentrifuge tube, 50 μM $CuSO_4$ was added, and incubation was continued for 5 min. The cleavage was activated by adding ascorbate (pH 7.4) to 30 mM and 1 μL of 30% H_2O_2. After 20 min, the reaction was terminated by adding neocuproine to a final concentration of 5 mM.

Purification of Subunit a. After reaction, membrane vesicles or whole cells were resuspended in extraction buffer (200 mM Tris-HCl (pH 8.0), 1.5% octyl glucoside, 0.1% deoxycholate, 0.5% cholate, 10 mM β-mercaptoethanol, 10 mM imidazole, and 1% Tween 20). The samples were incubated with agitation for 1 h at 4 °C and centrifuged at 14 000 rpm for 10 min in a microcentrifuge. The supernatant was added to 0.3 mL (0.15 mL for extracts from whole cells) of Ni−NTA resin that had been previously equilibrated in the extraction buffer. The mixture was incubated with agitation for 45 min at room temperature and centrifuged for 1 min at 14 000 rpm. The resin was washed three times with 1 mL of wash buffer, consisting of equal volumes of extraction buffer and 200 mM Tris-HCl (pH 8.0). Subunit *a* was eluted by adding 0.25 mL of elution buffer (extraction buffer containing 1 M imidazole). The mixture was incubated at room temperature for 5 min and centrifuged at 14 000 rpm for 1 min. The supernatant containing the purified subunit *a* was collected and stored at −20 °C.

Factor Xa Protease Reaction and Standards. Factor Xa sites were introduced by cassette mutagenesis. For the largest fragment, T68, S69, and G70 were replaced by IEGR, the Factor Xa recognition site. For the intermediate fragment, I129, A130, E131, and H132 were replaced by IEGR. For the smallest fragment, IEGR was inserted after residue 177. All three constructs permitted growth on succinate minimal medium. Samples of purified subunit *a* with engineered protease sites were diluted 2-fold with 20 mM Tris-HCl (pH 8.0), 100 mM NaCl, and 2 mM $CaCl_2$. For every 20 μL of the diluted sample, 1 μg of Factor Xa was added, and the samples were incubated overnight at room temperature.

MPB Detection and Immunoblotting. Samples of purified subunit *a* were subjected to SDS−polyacrylamide gel electrophoresis (12% or 15% acrylamide) and transferred to a PVDF membrane using a Trans-Blot apparatus (Bio-Rad) overnight at 30 V or 1 h at 100 V. The PVDF membrane was blocked with 5% low-fat powdered milk in 20 mM Tris-HCl (pH 7.5), 500 mM NaCl, and 0.05% Tween 20 (TBS/Tween 20) for 1 h and rinsed with TBS/Tween 20 three times. For MPB detection, the blocked membrane was incubated with avidin-conjugated alkaline phosphatase for 2 h, rinsed three times in TBS/Tween 20, and developed for color according to the manufacturer's instructions. For subunit *a* detection, the blocked PVDF membrane was incubated at room temperature for 2 h with mouse anti-HA antibody (50 μg/mL). After washing three times with TBS/Tween 20, it was incubated with goat anti-mouse IgG-alkaline phosphatase conjugate at a dilution of 1:1000 for 1 h. After another three washings with TBS/Tween 20, color was developed as described above. For subunit *b* detection, the blocked membrane was incubated at room temperature for 2 h with *b*-antibody at a dilution of 1:1000. After washing three times with TBS/Tween 20, it was incubated with goat anti-mouse IgG-alkaline phosphatase conjugate at a dilution of 1:1000 for 1 h. After another three washings with TBS/Tween 20, color was developed as described above. For subunit *c* detection, the blocked membrane was incubated at room temperature for 2 h with *c*-antibody at a dilution of 1:5000. After washing three times with TBS/Tween 20, it was incubated with goat anti-rabbit IgG-alkaline phosphatase conjugate at a dilution of 1:1000 for 1 h. After another three washings with TBS/Tween 20, color was developed as described above.

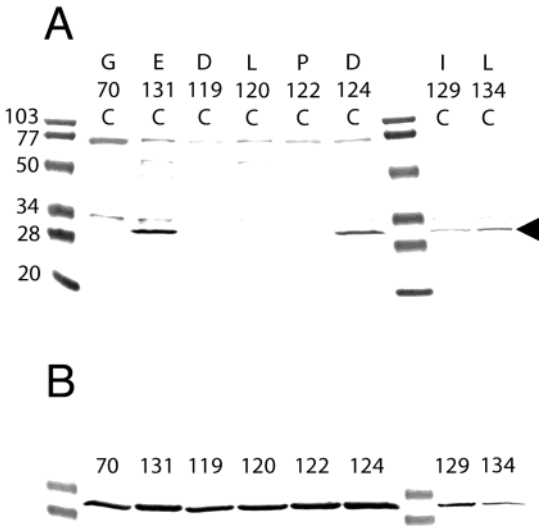

FIGURE 2: Labeling of subunit *a* from the periplasmic surface: residues 119, 120, 122, 124, 129, and 134. (A) Protein standards in kD are indicated at the left. MPB labeling in whole cells of G70C, E131C, D119C, L120C, P122C, D124C, I129C, and L134C is shown. The position of subunit *a* is indicated by the arrowhead. (B) Immunoblot of the samples in panel A.

RESULTS

In previous work (*19*, *21*) only three residues in the region between transmembrane spans 2 and 3 had been tested for accessibility to MPB: P127, Y128, and E131. In this study 18 additional cysteine substitution mutants were constructed at sites in this region, between residues 119 and 146. All mutants grew in succinate minimal medium, indicating the ability to carry out oxidative phosphorylation, although D119C grew poorly. Single-cysteine constructs of subunit *a*, which contains no naturally occurring cysteine, were tested for labeling in partially permeabilized whole cells, as described previously (*21*). The results are presented in Figures 2−4, in which panel A shows labeling by MPB and panel B shows immunoblotting for subunit *a*. In Figure 2 residues D119, L120, P122, D124, I129, and L134 are shown, along with control residues G70 and E131. Residue G70C has been shown to label only from the cytoplasmic surface and is included to demonstrate integrity of the plasma membrane (*21*). Residue E131 is a positive control that has been shown to be accessible from the periplasmic surface (*19*). In this experiment E131, D124, I129, and L134 are

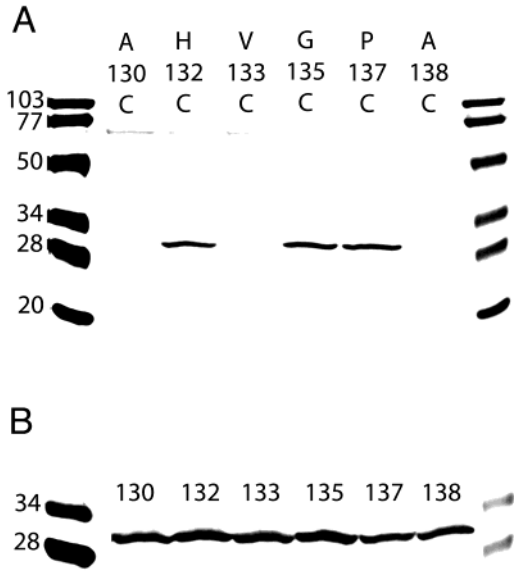

FIGURE 3: Labeling of subunit *a* from the periplasmic surface: residues 130, 132, 133, 135, 137, and 138. (A) Protein standards in kD are indicated at the left. MPB labeling in whole cells of A130C, H132C, V133C, G135C, P137C, and A138C is shown. (B) Immunoblot of the samples in panel A.

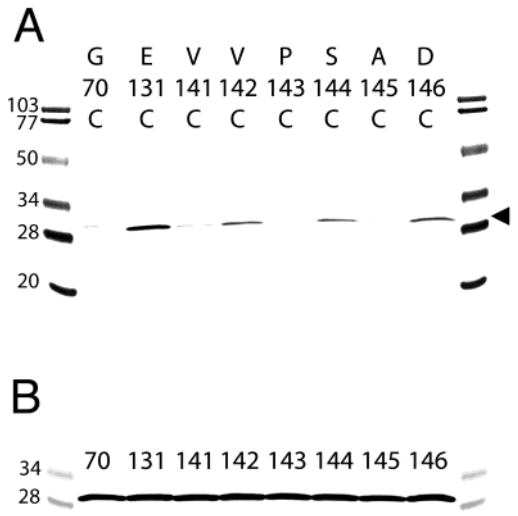

FIGURE 4: Labeling of subunit *a* from the periplasmic surface: residues 141−146. (A) Protein standards in kD are indicated at the left. MPB labeling in whole cells of G70C, E131C, V141C, V142C, P143C, S144C, A145C, and D146C is shown. The position of subunit *a* is indicated by the arrowhead. (B) Immunoblot of the samples in panel A.

shown to be accessible from the periplasm. In Figure 3, residues H132, G135, and P137 are shown to be accessible from the periplasm, while residues A130, V133, and A138 are not accessible. In Figure 4 the results indicate that V142, S144, and D146 are accessible from the periplasm, while residues V141, P143, and A145 are not accessible.

Initially, the chemical protease reaction was attempted in partially permeabilized cells, analogous to the procedures used above for labeling by MPB. In this case, the BAP was intended to attach covalently to subunit *a* through a unique cysteinyl residue. It was expected that fragmentation of the protein would reflect the location of the particular cysteinyl residue to which the reagent was attached. It was found that using this procedure, it was possible to generate fragments of wild-type subunit *a*, independent of the presence of

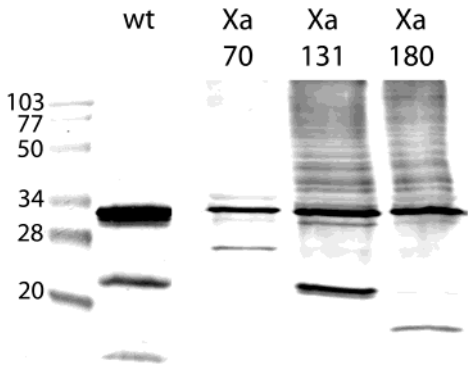

FIGURE 5: BAP-mediated proteolysis of wild-type subunit *a* in whole cells. Protein standards in kD are indicated at the left. Lane 2 contains wild-type (wt) subunit *a* purified by Ni−NTA after treatment of whole cells for proteolysis. Lane 3 contains Factor Xa-treated subunit *a* with an engineered site near residue 70. Lane 4 contains Factor Xa-treated subunit *a* with an engineered site near residue 131. Lane 5 contains Factor Xa-treated subunit *a* with an engineered site near residue 180.

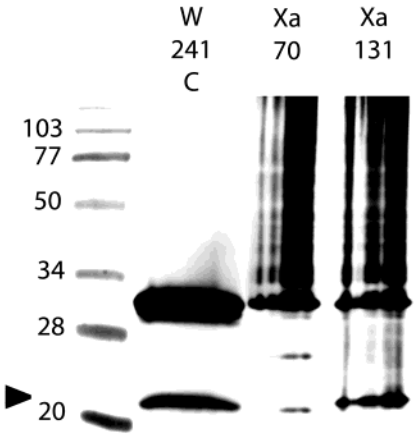

FIGURE 6: BAP-mediated proteolysis of W241C. Protein standards in kD are indicated at the left. Lane 2 contains W241C subunit *a* detergent-solubilized, reacted with BAP, activated for proteolysis, and purified by Ni−NTA. Its proteolytic fragment is indicated by the arrowhead at the left. Lane 3 contains Factor Xa-treated subunit *a* with an engineered site near residue 70. Lane 4 contains Factor Xa-treated subunit *a* with an engineered site near residue 131.

cysteinyl residues. As shown in Figure 5, one fragment is nearly full-length subunit *a*, and the other two are smaller. To estimate the size of these fragments, Factor Xa sites were introduced into subunit *a* at three different positions. They correspond to the carboxyl-terminal ends of transmembrane spans 2, 3, and 4, at the approximate positions 70, 131, and 177, respectively. The results of digestion by Factor Xa show unique bands in each case that reflect the distance of the protease site from the carboxyl-terminus, where the HA epitope is located. The mid-sized fragment from wild-type subunit *a* is seen to be similar in size to the 131 standard.

An alternative approach was developed to eliminate proteolysis of subunit *a* in the absence of cysteinyl residues. Subunit *a* was solubilized in detergent before the proteolytic reactions were initiated. The following residues were tested: 39, 43, 44, 119, 120, 141−145, 226−228, 230−232, 238, 240−242, 244, and 246. The most significant level of proteolysis was seen with W241C, which occurred to an extent of as much as 15%, as shown in Figure 6, lane 2. The Factor Xa control in lane 4 indicates that the proteolysis occurred near the carboxyl-terminal end of transmembrane

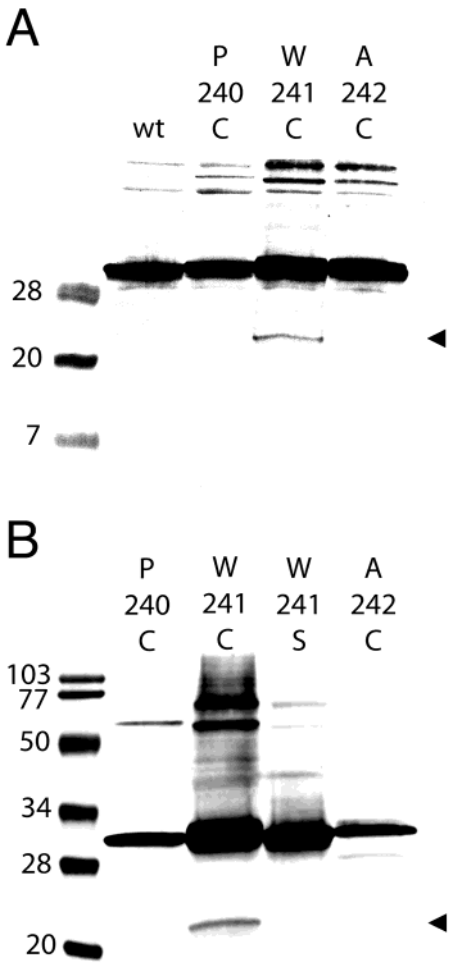

FIGURE 7: BAP mediated proteolysis of W241C with controls. Protein standards in kD are indicated at the left. The proteolytic fragment of subunit *a* is indicated by an arrowhead at the right. (A) Lane 1 contains protein standards. Lane 2 contains wild-type (wt) subunit *a*. Lane 3 contains P240C. Lane 4 contains W241C. Lane 5 contains A242C. (B) Lane 1 contains protein standards. Lane 2 contains P240C. Lane 3 contains W241C. Lane 4 contains W241S. Lane 5 contains A242C. All samples were detergent-solubilized, reacted with BAP, activated for proteolysis, purified by Ni−NTA, and detected by anti-HA.

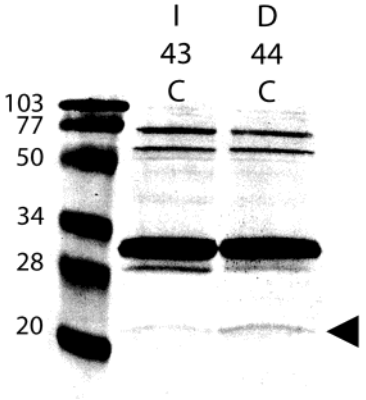

FIGURE 8: BAP-mediated proteolysis of I43C and D44C. Protein standards in kD are indicated at the left. The proteolytic fragment of subunit *a* is indicated by the arrowhead at the right. Lane 1 contains protein standards. Lane 2 contains I43C. Lane 3 contains D44C. Both samples were detergent-solubilized, reacted with BAP, activated for proteolysis, purified by Ni−NTA, and detected by anti-HA.

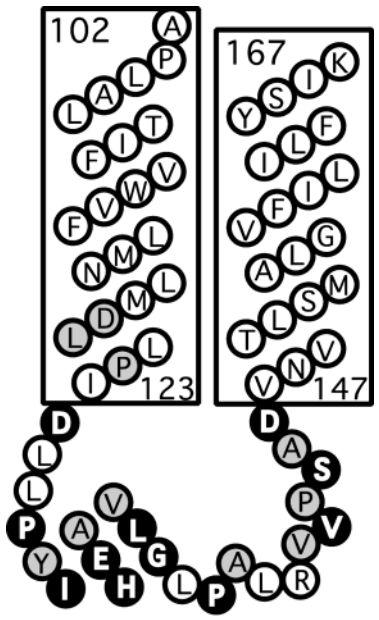

FIGURE 9: Model of the periplasmic loop between transmembrane spans 2 and 3 of subunit *a*. Residues that were labeled by MPB in PMBN-treated whole cells are noted as black circles with white lettering. Residues that were found to be inaccessible to MPB are shaded gray. Other residues, not tested, are white circles.

span 2. The results of several controls are shown in Figure 7. Panel 7A shows that wild type (lane 2), 240C (lane 3), and 242C (lane 5) do not generate proteolytic fragments. Panel 7B shows that an alternative mutation at residue 241, W241S, also does not generate a proteolytic fragment. Figure 8 shows the results of proteolysis with I43C (lane2) and D44C (lane3). Both positions generate two fragments, one nearly identical in size to that generated from W241C and one slightly shorter than the full-length subunit *a*.

DISCUSSION

The results of labeling with MPB presented here serve to better define the periplasmic ends of transmembrane spans 2 and 3 of subunit *a* of the *E. coli* ATP synthase. These results, as well as previous work, helped define sites for testing the chemical protease procedure, which identified several interactions between transmembrane spans.

The periplasmic loop between transmembrane spans 2 and 3 is now known to contain at least 23 residues, from D124 to D146. In previous work (*19*, *21*) three positions in this loop were examined by MPB labeling. Residues P127 and E131 were found to be accessible to labeling, while Y128 was not accessible. In this study, 15 additional residues were tested, with nine found to be accessible and six not accessible to MPB labeling. Five other residues between D124 and D146 were not tested. These results are summarized in Figure 9, in which accessible residues are colored black, inaccessible residues are colored gray, and untested ones are white. The pattern of labeling is consistent with a surface connection, in which about half of the residues are accessible. The periodicity of labeling does not match that predicted for a surface α-helix, except for the segment from 130 to 135.

These results indicate that there are only four ionizable residues that are found within the transmembrane spans of the *E. coli* subunit *a* near the periplasmic surface. They include D44 in transmembrane span 1, D119 in span 2, E219 in span 4, and H245 in span 5. The latter two have been

implicated in proton translocation activity (*23*, *25*, *26*, *35*, *36*), based on mutagenesis and sequence conservation, although E219 is known to tolerate several substitutions (*36*, *37*). The former two have been much less extensively studied by mutagenesis (*20*, *38*, *39*) and are not so highly conserved.

Metal chelate mediated chemical proteolysis using derivatives of 1,10-phenanthroline has been successfully used in studies of *lac* permease (*31*) and rhodopsin (*40*). The rationale of such experiments is that if the phenanthroline is attached to a particular site in the protein through its reaction with a free sulfhydryl group, the subsequent oxidative cleavage will be at a site in the polypeptide chain that is near the sulfhydryl group in the folded protein. This method offers an approach to learn about the proximity and orientation of transmembrane helices. The results with *lac* permease have been confirmed using several different approaches (*41*), while the crystal structure of rhodopsin has confirmed those studies (*42*). The results presented here indicate that transmembrane span 5 is near transmembrane span 2, with W241 of span 5 oriented toward span 2. In addition, both residues I43 and D44 of transmembrane span 1 must be oriented toward transmembrane span 2. These latter sites also generated a second fragment that was nearly full length, suggesting that the reagent was able to contact the amino-terminal region of the protein and therefore the sites must be near the periplasmic surface.

Previous studies have identified numerous second site suppressors of mutations in subunit *a*, primarily of residues E219 and H245. Studies by Cain and colleagues (*23*, *30*) have found suppression, to various extents, of H245 mutations at both positions 218 and 219. Since these residues are all found in the interior regions of adjacent transmembrane spans, it is likely that they are close in space in the folded protein. Another suppressor of a H245 mutation was identified (*20*), at position D119, shown here to be an inaccessible residue of transmembrane span 2. The proximity of these two residues in the folded protein is supported by the proteolysis results presented here. W241 is likely to be about one turn of an α-helix from H245, toward the periplasmic surface, and the site of cleavage in transmembrane span 2 is also likely to be toward the periplasmic surface from D119. Suppressors of E219C (*20*) have been identified at position 145, and suppressors of E219H (*29*) have been identified at position 140. Results presented here indicate that residues A145 and R140 are in the periplasmic loop, while E219 is buried in the membrane, and therefore these suppressors must be acting indirectly. These results are summarized in two possible models of helix packing in Figure 10. Each model is a view from the cytoplasm with R210 pointing out toward the ring of *c* subunits. In model A the connectivity of the helices is the opposite of bacteriorhodopsin. After orienting W241 (span 5) and I43 and D44 (span 1) toward transmembrane span 2, it allows for close contact of H245 (span 5), D119 (span 2), and E219 (span 4). In model B, the connectivity of the helices is the same as bacteriorhodpsin. Both models incorporate a sequential ordering of the transmembrane spans, with ionizable residues, aside from R210, pointing toward the interior of the bundle.

One consequence of the position of E219, i.e., 2.5 turns of an α-helix away from the critical residue R210, is that it is likely to interact with residues from other transmembrane spans. The protonation of such a network of residues could then be communicated immediately to the R210, allowing protonation of the *c* subunit at D61.

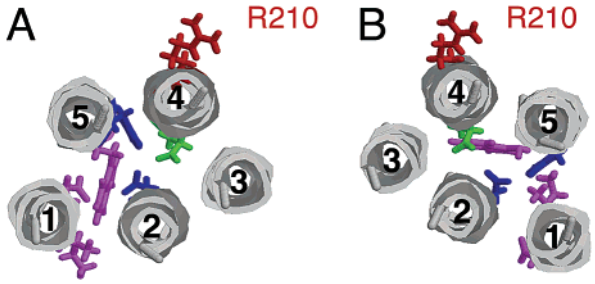

FIGURE 10: Models for helix packing in subunit *a*. Both panels are colored in the same way. R210 is colored red and is positioned to contact the ring of *c* subunits. W241 of span 5 and I43 and D44 of span 1 are colored magenta. Those are the sites that lead to proteolysis of span 2. H245 of span 5 and D119 of span 2 are colored blue. They are likely to be in close contact. E219 of span 4 is colored green. (A) A counterclockwise arrangement of the spans as viewed from the cytoplasm. (B) A clockwise arrangement of the spans as viewed from the cytoplasm.

Several comments can be made about the method of metal chelate mediated proteolysis. First, while the BAP-dependent proteolysis of subunit *a* in whole cells failed to show specificity for cysteinyl residues, it seemed to react with all three periplasmic regions of the protein. The enhanced reactivity could be due to accumulation of BAP in the periplasm and to the relatively oxidizing environment of this compartment. This whole-cell approach might be applicable for identification of the number of transmembrane spans of any inner membrane protein with an epitope tag at one of the termini. Second, reaction with detergent solubilized subunit *a* did not lead to extensive proteolysis but was in fact confined to just three residues. This might be due to the close packing of helices in a protein, such as subunit *a*, that is involved in proton transport. Mutagenesis of tryptophan to cysteine might have served to generate a large enough cavity for the BAP to approach the sulfhydryl group. The analysis of the W241S mutant showed that proteolysis was not simply a consequence of an altered conformation due to mutagenesis of the tryptophan.

REFERENCES

1. Capaldi, R. A., and Aggeler, R. (2002) *Trends Biochem. Sci. 27*, 154−160.
2. Foster, D. L., and Fillingame, R. H. (1982) *J. Biol. Chem. 257*, 2009−2015.
3. Abrahams, J. P., Leslie, A. G. W., Lutter, R., and Walker, J. E. (1994) *Nature 370*, 621−628.
4. Gibbons, C., Montgomery, M. G., Leslie, A. G., and Walker, J. E. (2000) *Nat. Struct. Biol. 7*, 1055−10561.
5. Menz, R. I., Walker, J. E., and Leslie, A. G. (2001) *Cell 106*, 331−341.
6. Yasuda, R., Noji, H., Yoshida, M., Kinosita, K., Jr., and Itoh, H. (2001) *Nature 410*, 898−904.
7. Noji, H., Yasuda, R., Yoshida, M., and Kinosita, K., Jr. (1997) *Nature 386*, 299−302.
8. Kato-Yamada, Y., Noji, H., Yasuda, R., Kinosita, K., Jr., and Yoshida, M. (1998) *J. Biol. Chem. 273*, 19375−19377.
9. Dunn, S. D. (1992) *J. Biol. Chem. 267*, 7630−7636.
10. McLachlin, D. T., and Dunn, S. D. (1997) *J. Biol. Chem. 272*, 21233−21239.
11. Sorgen, P. L., Bubb, M. R., McCormick, K. A., Edison, A. S., and Cain, B. D. (1998) *Biochemistry 37*, 923−932.
12. Revington, M., McLachlin, D. T., Shaw, G. S., and Dunn, S. D. (1999) *J. Biol. Chem. 274*, 31094−31101.
13. Revington, M., Dunn, S. D., and Shaw, G. S. (2002) *Protein Sci. 11*, 1227−1238.

14. Dmitriev, O., Jones, P. C., Jiang, W., and Fillingame, R. H. (1999) *J. Biol. Chem. 274*, 15598−15604.
15. Girvin, M. E., Rastogi, V. K., Abildgaard, F., Markley, J. L., and Fillingame, R. H. (1998) *Biochemistry 37*, 8817−8824.
16. Seelert, H., Poetsch, A., Dencher, N. A., Engel, A., Stahlberg, H., and Muller, D. J. (2000) *Nature 405*, 418−419.
17. Stahlberg, H., Muller, D. J., Suda, K., Fotiadis, D., Engel, A., Meier, T., Matthey, U., and Dimroth, P. (2001) *EMBO Rep. 2*, 229−233.
18. Jiang, W., Hermolin, J., and Fillingame, R. H. (2001) *Proc. Natl. Acad. Sci. U.S.A. 98*, 4966−4971.
19. Long, J. C., Wang, S., and Vik, S. B. (1998) *J. Biol. Chem. 273*, 16235−16240.
20. Valiyaveetil, F. I., and Fillingame, R. H. (1998) *J. Biol. Chem. 273*, 16241−16247.
21. Wada, T., Long, J. C., Zhang, D., and Vik, S. B. (1999) *J. Biol. Chem. 274*, 17353−17357.
22. Long, J. C., DeLeon-Rangel, J., and Vik, S. B. (2002) *J. Biol. Chem. 277*, 27288−27293.
23. Cain, B. D., and Simoni, R. D. (1988) *J. Biol. Chem. 263*, 6606−6612.
24. Cain, B. D., and Simoni, R. D. (1989) *J. Biol. Chem. 264*, 3292−3300.
25. Lightowlers, R. N., Howitt, S. M., Hatch, L., Gibson, F., and Cox, G. (1988) *Biochim. Biophys. Acta 933*, 241−248.
26. Lightowlers, R. N., Howitt, S. M., Hatch, L., Gibson, F., and Cox, G. B. (1987) *Biochim. Biophys. Acta 894*, 399−406.
27. Jiang, W., and Fillingame, R. H. (1998) *Proc. Natl. Acad. Sci. U.S.A. 95*, 6607−6612.
28. Vik, S. B., Patterson, A. R., and Antonio, B. J. (1998) *J. Biol. Chem. 273*, 16229−16234.
29. Howitt, S. M., Lightowlers, R. N., Gibson, F., and Cox, G. B. (1990) *Biochim. Biophys. Acta 1015*, 264−268.
30. Hartzog, P. E., and Cain, B. D. (1994) *J. Biol. Chem. 269*, 32313−32317.
31. Wu, J., Perrin, D. M., Sigman, D. S., and Kaback, H. R. (1995) *Proc. Natl. Acad. Sci. U.S.A. 92*, 9186−9190.
32. Vik, S. B., Cain, B. D., Chun, K. T., and Simoni, R. D. (1988) *J. Biol. Chem. 263*, 6599−6605.
33. Humbert, R., Brusilow, W. S., Gunsalus, R. P., Klionsky, D. J., and Simoni, R. D. (1983) *J. Bacteriol. 153*, 416−422.
34. Hartzog, P. E., and Cain, B. D. (1993) *J. Bacteriol. 175*, 1337−1343.
35. Cain, B. D., and Simoni, R. D. (1986) *J. Biol. Chem. 261*, 10043−10050.
36. Valiyaveetil, F. I., and Fillingame, R. H. (1997) *J. Biol. Chem. 272*, 32635−32641.
37. Hatch, L. P., Cox, G. B., and Howitt, S. M. (1998) *Biochim. Biophys. Acta 1363*, 217−223.
38. Howitt, S. M., Gibson, F., and Cox, G. B. (1988) *Biochim. Biophys. Acta 936*, 74−80.
39. Paule, C. R., and Fillingame, R. H. (1989) *Arch. Biochem. Biophys. 274*, 270−284.
40. Gelasco, A., Crouch, R. K., and Knapp, D. R. (2000) *Biochemistry 39*, 4907−4914.
41. Kaback, H. R., Voss, J., and Wu, J. H. (1997) *Curr. Opin. Struct. Biol. 7*, 537−542.
42. Teller, D. C., Okada, T., Behnke, C. A., Palczewski, K., and Stenkamp, R. E. (2001) *Biochemistry 40*, 7761−7772.

BI026649T